San Andreas fault geometry through the San Gorgonio Pass, California

Laura Dair, Michele L. Cooke
Department of Geosciences, University of Massachusetts, Amherst, Massachusetts 01003, USA

ABSTRACT

Three-dimensional numerical models are needed to investigate the role of nonvertical strike-slip fault segments on the deformation within restraining bends. Numerical models simulate geologic deformation of two alternative three-dimensional present-day configurations for the San Andreas fault through the restraining bend within the San Gorgonio Pass region (SGPR) in Southern California. Both models produce decreasing strike-slip rates southward along the San Bernardino strand of the San Andreas fault, similar to geologic data. The north-dipping San Andreas fault model better matches the available strike-slip data as well as the geologic uplift data for the southern San Bernardino Mountains than the vertical San Andreas fault model. We conclude that a north-dipping fault configuration is preferred for models of the San Andreas fault in the SGPR. The complexity of the active fault geometry at the SGPR promotes the transfer of strike slip from the San Andreas fault to the nearby but unconnected San Jacinto fault. Slip rates and uplift patterns are sensitive to fault geometry within strike-slip restraining bends.

INTRODUCTION

Restraining bends along strike-slip faults are traditionally believed to be composed of vertical strike-slip fault segments that curve along strike. However, two of the best-known restraining bends, the Santa Cruz and the San Bernardino Mountains, California, may be associated with active nonvertical segments of the San Andreas fault (e.g., Allen, 1957; Anderson, 1990; Matti et al., 1992; Nicholson, 1996; Yule and Sieh, 2003; Carena et al., 2004). As geophysical studies reveal greater details of active strike-slip fault geometry within restraining bends, we require three-dimensional models that can fully investigate the contribution of nonvertical strike-slip faults to local deformation.

At the San Gorgonio Pass region (SGPR) of Southern California, the San Andreas fault steps left in a restraining bend that has evolved into a complex network of active and formerly active, dipping and vertical, three-dimensionally irregular fault surfaces (Fig. 1; e.g., Matti et al., 1985). Although field and geophysical investigations reveal active north-dipping thrust faults through the SGPR (e.g., Allen, 1957; Matti et al., 1992; Nicholson, 1996; Yule and Sieh, 2003; Carena et al., 2004; Langenheim et al., 2005), crustal deformation and earthquake rupture models simplify the San Andreas fault as vertical through this region (e.g., Meade and Hager, 2005; Olsen et al., 2006; Smith and Sandwell, 2006). Within these simplified fault models, slip vectors are primarily strike slip, and the models neglect the reverse slip documented on the north-dipping San Gorgonio thrust (Yule and Sieh, 2003). As a consequence, physical aspects of earthquake rupture dynamics and the regional seismic hazard may go uncharacterized. Models of the southern San Andreas fault with geologically realistic geometry, which are now possible at relatively high resolutions, may lead to more accurate assessment of earthquake hazards for southern California. Such models are of timely importance as the segments of the southern San Andreas fault south of the Cajon Pass have not slipped substantially enough to release accumulated strain, and may be nearing the end of their recurrence intervals (e.g., Yule et al., 2001; Weldon et al., 2004, 2005).

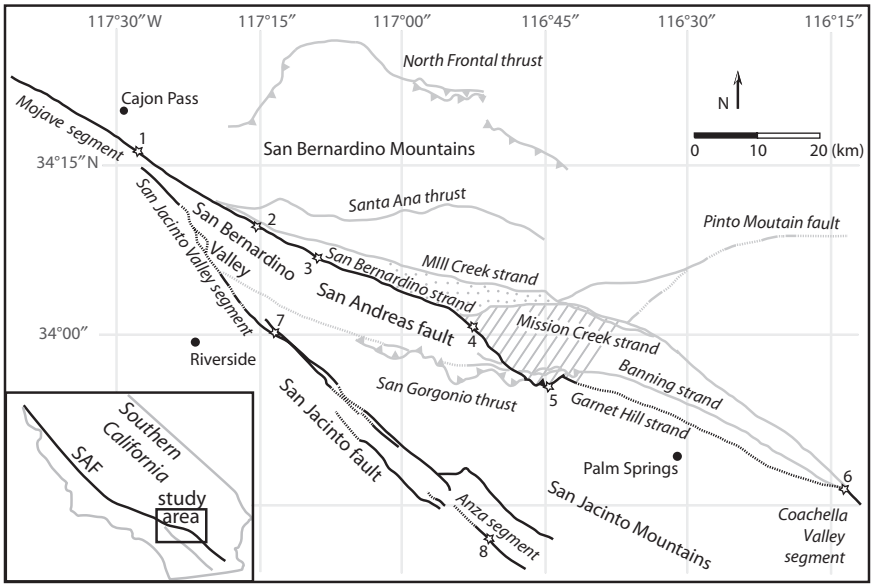

Figure 1. Fault trace map of San Gorgonio Pass region. Model simulations of active faulting only include black faults. Gray faults are secondary. Stars indicate locations of geologic study sites that have yielded slip rates. Dashed lines indicate faults that have no surface trace. Stippled section is Yucaipa Ridge block; cross-hachured section is Morongo block of San Bernardino Mountains. SAF—San Andreas fault. Site 1, Cajon Pass—Weldon and Sieh (1985); site 2, Badger Canyon—McGill (2007); site 3, Plunge Creek—McGill et al. (2006); site 4, Burro Flats—Orozco (2004); site 5—Yule et al. (2001); site 6—Behr et al. (2007); site 7—Kendrick et al. (2002); site 8—Rockwell et al. (1990), Rockwell (2006) (modified from Matti et al. 1992).

We use the boundary element method (BEM) to numerically simulate geologic-time-scale crustal deformation of two different San Andreas fault configurations through the SGPR. The BEM modeling technique uses a triangular mesh to accurately replicate three-dimensionally irregular fault surfaces. Using this mesh, we have developed the first crustal deformation model of the southern San Andreas fault that incorporates geologically constrained north-dipping fault segments. We compare the model results to geologic observations and offer a preferred

fault configuration for the San Andreas fault through the restraining bend of the SGPR. Our study reveals the sensitivity of slip distribution and uplift pattern to fault configuration through a restraining bend and may guide future models in other regions.

GEOLOGIC UPLIFT AND SLIP RATES

The SGPR contains a complex network of strike-slip and thrust faults. Between the vertical strike-slip segments of the San Andreas fault north and south of the San Gorgonio Pass (i.e., the San Bernardino strand and Coachella Valley segment of the San Andreas fault), Yule and Sieh (2003) documented two active north-dipping fault strands of the San Andreas, the San Gorgonio thrust and the Garnet Hill fault (Fig. 1). Microseismicity in the region suggests that these faults maintain their north dip of 45º–85° at depth (Carena et al., 2004). Both the observed and interpreted north dip on these two faults refute the presence of a vertical through-going strand of the San Andreas fault within the SGPR (Fig. 1; Yule and Sieh, 2003; Carena et al., 2004).

Low-temperature thermochronometry at the Yucaipa Ridge, located between the now inactive Mill Creek strand and the active San Bernardino strand of the San Andreas fault, indicates ~3–6 km of uplift in the past 1.8 m.y. (Spotila et al., 2001). While the time-averaged uplift rate of the Yucaipa Ridge is 1.6–3.3 mm/yr, uplift was faster ca. 1.5 Ma than in the recent past (Spotila, et al., 2001). Offset markers across the San Gorgonio thrust show 1 mm/yr relative uplift over the past 13 k.y. (Yule and Sieh, 2003). Spatial variations in uplift rates are expected due to local fault geometry.

Geologic studies have revealed variable strike-slip rates along both the San Andreas fault and San Jacinto fault within the SGPR. Near the Cajon Pass, Weldon and Sieh (1985) found 24.5 ± 3.5 mm/yr strike slip along the San Andreas fault. Southward, rates decrease along the San Bernardino strand to 11–16 mm/yr at Badger Canyon (McGill et al., 2007) to 3–17 mm/yr at Plunge Creek (McGill et al., 2006), and to 2.6–7.0 mm/yr at Burro Flats (Orozco, 2004). Where the San Bernardino strand intersects the San Gorgonio thrust and Garnet Hill strand of the San Andreas fault, the strike-slip rate decreases to 5.7 ± 0.8 mm/yr (Yule et al., 2001). The northern Coachella Valley segment of the San Andreas fault slips 9–15 mm/yr (Behr et al., 2007). Along the San Jacinto fault, strike-slip rates vary from >20 mm/yr at site 7 (Fig. 1; Kendrick et al., 2002) to >9.2 mm/yr from alluvial fan offsets (Rockwell et al., 1990). In addition to strike-slip rates in the region, Yule and Sieh (2003) found a minimum of 2.5 mm/yr reverse slip on the San Gorgonio thrust.

SAN ANDREAS FAULT MODEL ALTERNATIVES

Two different fault geometries for active faults in the SGPR were created based on the Southern California Earthquake Center Community Fault Model (CFM), a compilation of active faults in southern California (Plesch et al., 2007). The first model has a simplified vertical fault geometry for the San Andreas fault within the SGPR. The second model follows the preferred configuration of the CFM (Carena et al., 2004; Plesch et al., 2007), and includes a 45º–85° north-dipping Garnet Hill strand and San Gorgonio thrust (Fig. 2B). In both models, the faults are freely slipping to a depth of 35 km, where they intersect a horizontal freely slipping crack that decouples crustal deformation from the modeled half space. Within the model, discrete fault surfaces below the seismogenic crust simulate distributed deformation expected at these depths. Rather than prescribing slip along the faults within the SGPR, the weak faults of our model slip and interact in response to regional plate motions of 45 mm/yr N52°W right-lateral displacement (e.g., Bennett et al., 1999; Shen et al., 2003) applied at the edges of the horizontal crack. The setup of the models is further described in the supplement to this paper (see the GSA Data Repository[1]).

MODELED VERTICAL DEFORMATION PATTERNS

The surface uplift maps reveal significant differences between the vertical and north-dipping San Andreas fault models (Fig. 3). The vertical configuration produces far less relative surface uplift than the north-dipping configuration. The greater uplift rates on the hanging wall of the north-dipping San Andreas fault model are due to significant reverse slip rates on the dipping fault segments. The average reverse slip rate on the modeled San Gorgonio thrust, 3.6 mm/yr, matches geologic observations (>2.5 mm/yr; Yule and Sieh, 2003). The north-dipping model has the greatest relative uplift in the areas of the Yucaipa Ridge block and the Morongo block (Fig. 1), which have been uplifted at higher rates than the surrounding area (Spotila et al., 2001). The relative uplift rates produced by the north-dipping fault model at the Yucaipa Ridge (~1.6–1.9 mm/yr) are within the lower half of time-averaged geologic uplift rates (1.6–3.3 mm/yr), also consistent with slower uplift in times later than 1.5 Ma (Spotila et al., 2001). In contrast, the vertical fault model produces only ~0.4–0.7 mm/yr of relative uplift and cannot account for the geologic uplift rates. Vertical models with strike-slip rates as fast as 28 mm/yr though the restraining bend can produce 1–3 mm/yr of uplift adjacent to the fault (Smith and Sandwell, 2003); however, such slip rates greatly exceed the geologic observations within the restraining bend in the SGPR (Fig. 4). Both of our models produce subsidence

[1]GSA Data Repository item 2009034, numerical methodology, is available online at www.geosociety.org/pubs/ft2009.htm, or on request from editing@geosociety.org or Documents Secretary, GSA, P.O. Box 9140, Boulder, CO 80301, USA.

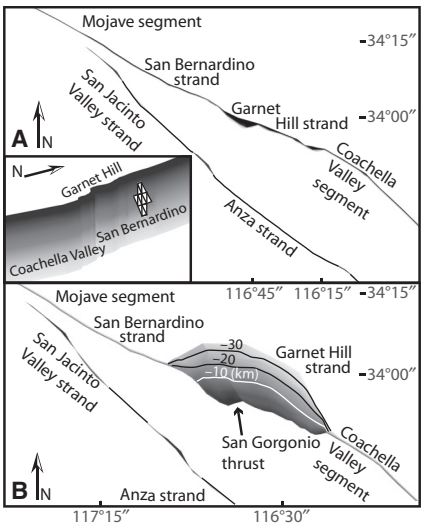

Figure 2. Map views of San Andreas fault geometries. Lighter shades indicate deepening depths to 35 km. Structure contours are overlain on dipping segments. A: Vertical; inset within shows section of mesh used for fault surfaces. B: North dipping.

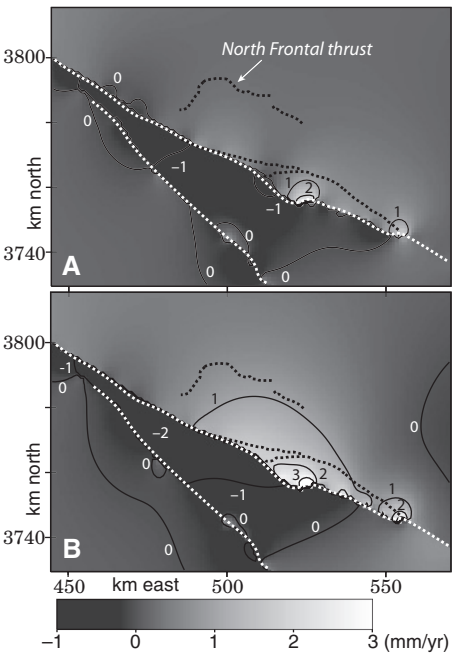

Figure 3. Vertical deformation maps for both models. Unlike vertical model, dipping models produce uplift within region of southern San Bernardino Mountains (e.g., Yucaipa Ridge and Morongo blocks; Fig. 1). Dotted lines are faults (Fig. 1).

>1 mm/yr within the San Bernardino Basin, which is consistent with depositional rates of ~1 mm/yr in this valley (Matti and Morton, 1993).

SITE-SPECIFIC GEOLOGIC SLIP RATES

We also compare the modeled slip rates at the Earth's surface with geologic rates obtained through specific paleoseismic and geomorphic studies (Fig. 4). The modeled strike-slip rates along the San Bernardino strand of the San Andreas fault decrease to the southeast and correlate well with geologic slip rates. However, the vertical San Andreas fault model overestimates right-lateral slip rates at more sites along the San Bernardino strand of the San Andreas fault than the north-dipping model. Again, the north-dipping fault configuration shows a more favorable comparison to geologic observations than the vertical fault model. The strike-slip rate data along the San Jacinto fault cannot distinguish between the models due to the simplification of the modeled San Jacinto fault.

The geologically observed, and model reproduced, pattern of decreasing slip rate to the southeast along the San Bernardino strand of the San Andreas fault demonstrates the significant spatial variability of slip rates along fault segments due to interaction with nearby faults. The discrepancy of some geologic slip rates on the San Bernardino fault segment with slip rates from geodetic block models (Meade and Hager, 2005) may reflect the inability of the block models to incorporate the region's geologic complexity.

SLIP TRANSFER: SAN ANDREAS FAULT TO SAN JACINTO FAULT

Right-lateral slip along the San Andreas fault is lowest for both models along the San Gorgonio thrust–Garnet Hill strand, which is the area of greatest geometric complexity. This decrease in strike-slip rate along the San Andreas fault occurs at the same distance from the Cajon Pass as the greatest strike-slip rates along the San Jacinto fault (Fig. 4). This suggests that, in the model, strike slip is transferred from the San Andreas fault to the San Jacinto fault even though the faults are not hard linked (i.e., connected). Within the models, the inefficiency of the restraining bend impedes strike slip along the San Andreas fault, allowing the San Jacinto fault to absorb the excess strike slip (Fig. 4). Slip can transfer between two separated faults as the shear stresses are transmitted through the intervening material, producing a soft link (e.g., Crider and Pollard, 1998; Roberts and Michetti, 2004). When slip cannot be accommodated on a fault due to an inefficient geometry, some of that slip is taken up by other faults and the remainder becomes off-fault deformation.

GEOMOPHOLOGY AND REGIONAL TRANSPRESSION

Although deformation is driven by N52°W right-lateral displacements at the edges of the model, the lack of applied regional transpression does not hinder the development of localized uplift in the north-dipping model. The contrasting uplift produced by the vertical and north-dipping San Andreas fault models indicates that dipping fault geometry can account for significant uplift without regional transpression. The inference that local fault configuration contributes to the San Bernardino Mountains uplift is consistent with the conclusions of several uplift studies in the region (e.g., Dibblee, 1975; Matti and Morton 1993; Spotila and Sieh, 2000; Spotila et al., 2007).

PREFERRED FAULT CONFIGURATION

The vertical San Andreas fault model fails to match the geologic uplift pattern, overestimates slip rates at several sites along the San Bernardino strand of the San Andreas fault, and neglects the geologic and seismic indications of active north-dipping faults in the SGPR. Of the two models, we favor the north-dipping geometry for the San Andreas fault through the SGPR.

Our results suggest that crustal deformation models for restraining bends that use only vertical faults will overestimate slip rates and underestimate off-fault deformation. The complexity of active faults through the SGPR may influence earthquake rupture scenarios because regions of fault surface complexity may be regions where ruptures initiate, terminate, or jump to other faults (e.g., Harris et al., 1991; Wald and Heaton, 1994). Earthquake rupture along the southern San Andreas fault may produce significant ground shaking within the metropolitan Los Angeles region (Olsen et al., 2006). Consequently, the constraints on fault geometry suggested here will help future rupture models of the southern San Andreas fault more accurately predict seismic hazards.

CONCLUSIONS

Our three-dimensional models confirm the geologic and geophysical evidence for north-dipping active fault segments along the San Andreas fault within the SGPR and demonstrate that nonvertical strike-slip segments can play a significant role in active deformation of restraining bends. Furthermore, incorporating geologic complexities, such as dipping fault surfaces, into numerical fault models, which is now more feasible than ever, increases the match between modeled results and geologic observations. For example, the uplift of the San Bernardino Mountains is better matched by active north-dipping faults within the restraining bend than by a vertical San Andreas fault. Similarly, the north-dipping San Andreas fault model better matches variable strike-slip rates at sites along the San Bernardino strand of the San Andreas fault. The match of the model results to the geologic observation of decreasing strike slip along the San Bernardino strand of the San Andreas fault highlights the value of geologic time scale models that do not prescribe fault slip rates

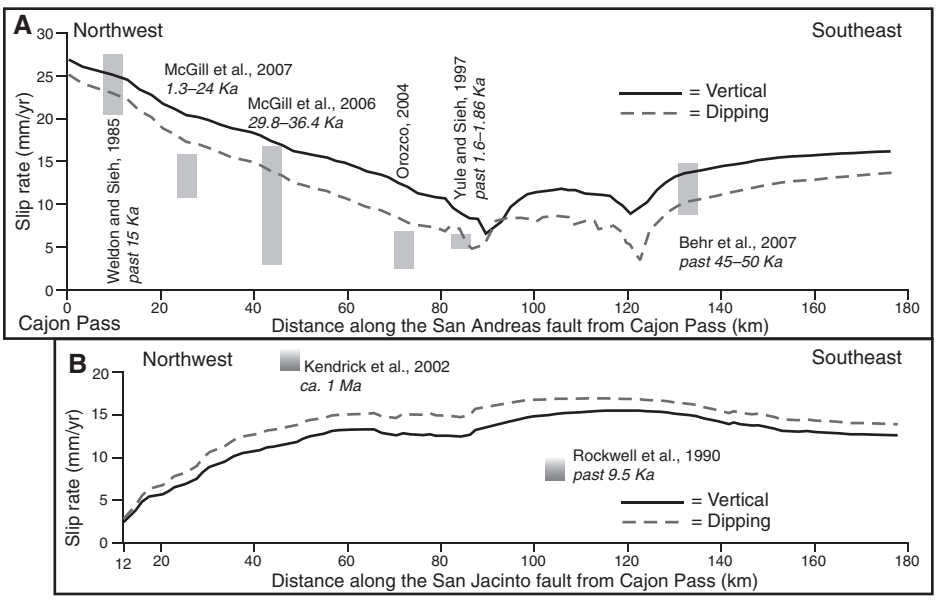

Figure 4. Surface strike-slip rates along fault traces within San Gorgonio Pass region. Graphs have been arranged so that the scales are the same and positioned according to distance from Cajon Pass. Northwestern half of plot A shows decreasing strike-slip rate along San Bernardino strand of San Andreas fault from Cajon Pass to San Gorgonio thrust. Vertical, continuous model has greater right-lateral slip rate along San Andreas fault and exceeds geologic slip rates at more sites than the north-dipping model. Vertical San Andreas fault model has slower strike-slip rates than the north-dipping model along San Jacinto fault in graph B. Gradational ranges indicate minimum slip rate estimates.

a priori. Within the models of the SGPR, the San Jacinto fault picks up some of the strike slip that is lost to the San Andreas fault in an effort to bypass the inefficient San Andreas fault geometry. This transfer occurs between soft-linked faults that have no physical connection. This study also reveals the sensitivity of uplift patterns and fault slip rates to fault geometry within restraining bends. Our results highlight the need for crustal deformation models of restraining bends to carefully consider nonvertical strike-slip fault geometry.

ACKNOWLEDGMENTS

We thank James Spotila, Bridget Smith-Konter, Doug Yule, and an anonymous reviewer for their constructive reviews. Funding for this research was provided by U.S. Geological Survey National Earthquake Hazards Reduction Program grant 8HQGR0041 and a grant from Southern California Earthquake Center (SCEC). This manuscript is SCEC publication 1160. IGEOSS provided Poly3D modeling software, and manipulation of fault surfaces was facilitated by use of 3DMove by Midland Valley Ltd.

REFERENCES CITED

Allen, C.R., 1957, San Andreas fault zone in the San Gorgonio Pass, southern California: Geological Society of America Bulletin, v. 68, p. 315–350, doi: 10.1130/0016–7606(1957)68[315:SAFZIS]2.0.CO;2.

Anderson, R.S., 1990, Evolution of the northern Santa Cruz Mountains by advection of crust past a San Andreas fault bend: Science, v. 249, 4967, p. 397–401.

Behr, W., Hudnut, K., Platt. J., Kendrick, K., Sharp, W., Fletcher K., Finkel, R., and Rood, D., 2007, A revised slip rate estimate for the Mission Creek–Coachella Valley strand of the southern San Andreas fault at Biskra Palms Oasis, Indio, California: Southern California Earthquake Center Annual Meeting, Proceedings with Abstracts, v. 17.

Bennett, R.A., Davis, J.L., and Wernicke, B.P., 1999, Present-day pattern of Cordilleran deformation in the western United States: Geology, v. 27, p. 371–374, doi: 10.1130/0091–7613(1999)027<0371:PDPOCD>2.3.CO;2.

Carena, S., Suppe, J., and Kao, H., 2004, Lack of continuity of the San Andreas fault in southern California: Three-dimensional fault models and earthquake scenarios: Journal of Geophysical Research, v. 109, B04313, doi: 10.1029/2003JB002643.

Crider, J.G., and Pollard, D.D., 1998, Fault linkage: Three-dimensional mechanical interaction between echelon normal faults: Journal of Geophysical Research, v. 103, no. B10, p. 24,373–24,391, doi: 10.1029/98JB01353.

Dibblee, T., 1975, Late Quaternary uplift of the San Bernardino Mountains of the San Andreas and related faults: California Division of Mines and Geology Special Report 118, p. 127–137.

Harris, R.A., Archuleta, R.J., and Day, S.M., 1991, Fault steps and dynamic rupture process: 2-D numerical simulations of a spontaneously propagating shear fracture: Geophysical Research Letters, v. 18, p. 893–896, doi: 10.1029/91GL01061.

Kendrick, K.J., Morton, D.M., Wells, S.G., and Simpson, R.W., 2002, Spatial and temporal deformation along the northern San Jacinto fault, southern California; implications for slip rates: Seismological Society of America Bulletin, v. 92, p. 2782–2802.

Langenheim, V.E., Jachens, R.C., Matti, J.C., Hauksson, E., Morton, D.M., and Christensen, A., 2005, Geophysical evidence for wedging in the San Gorgonio Pass structural knot, southern San Andreas fault zone, southern California: Geological Society of America Bulletin, v. 117, p. 1554–1572, doi: 10.1130/B25760.1.

Matti, J.C., and Morton, D.M., 1993, Paleographic evolution of the San Andreas fault in southern California: A reconstruction based on new cross-fault correlation, *in* Powell, R.E., et al., eds., The San Andreas fault system: Displacement, palinspastic reconstruction, and geologic evolution: Geological Society of America Memoir 178, p. 107–159.

Matti, J.C., Morton, D.M., and Cox, B.F., 1985, Distribution and geologic relations of fault systems in the vicinity of the central Transverse Ranges, southern California: U.S. Geological Survey Open-File Report 85–365, 23 p.

Matti, J.C., Morton, D.M., and Cox, B.F., 1992, The San Andreas fault system in the vicinity of the central Transverse Ranges province, southern California: U.S. Geological Survey Open-File Report 92–354, 52 p.

McGill, S., Weldon, R.J., II, Kendrick, K., and Owen, L., 2006, Late Pleistocene slip rate of the San Bernardino strand of the San Andreas fault in Highland: Possible confirmation of the low rate suggested by geodetic data: Seismological Research Letters, v. 77, no. 2, p. 279.

McGill, S., Kendrick, K., Weldon, R.J., II, and Owen, L., 2007, Pleistocene and Holocene slip rate of the San Andreas fault at Badger Canyon, San Bernardino, California: Southern California Earthquake Center Annual Meeting, Proceedings with Abstracts, v. 17.

Meade, B.J., and Hager, B.H., 2005, Block models of crustal motion in southern California constrained by GPS measurements: Journal of Geophysical Research, v. 110, B03403, doi: 10.1029/2004JB003209.

Nicholson, C., 1996, Seismic behavior of the Southern San Andreas fault zone in the Northern Coachella Valley, California: Comparison of the 1948 and 1986 earthquake sequences: Seismological Society of America Bulletin, v. 86, p. 1331–1349.

Olsen, K.B., Day, S.M., Minster, J.B., Cui, Y., Chourasia, A., Faerman, M., Moore, R., Maechling, P., and Jordan, T., 2006, Strong shaking in Los Angeles expected from southern San Andreas earthquake: Geophysical Research Letters, v. 33, L07305, doi: 10.1029/2005GL025472.

Orozco, A.A., 2004, Offset of a mid-Holocene alluvial fan near Banning, CA; constraints on the slip rate of the San Bernardino strand of the San Andreas fault [M.S. thesis]: University of California at Northridge, 56 p.

Plesch, A., and 27 others, 2007, Community fault model (CFM) for southern California: Seismological Society of America Bulletin, v. 97, p. 1793–1802, doi: 10.1785/0120050211.

Roberts, G.P., and Michetti, A.M., 2004, Spatial and temporal variations in growth rates along active normal fault systems: An example from the Lazio-Abruzzo Apennines, central Italy: Journal of Structural Geology, v. 26, p. 339–376, doi: 10.1016/S0191–8141(03)00103–2.

Rockwell, T., Loughman, C., and Merifield, P., 1990, Late Quaternary rate of slip along the San Jacinto fault zone near Anza, southern California: Journal of Geophysical Research, v. 95, no. B6, p. 8593–8605, doi: 10.1029/JB095iB06p08593.

Shen, Z.K., Agnew, D.C., King, R.W., Dong, D., Herring, T.A., Wang, M., Johnson, H., Anderson, G., Nikolaidis, R., van Domselaar, M., Hudnut, K.W., and Jackson, D.D., 2003, The SCEC crustal motion map, version 3.0: Los Angeles, California, Southern California Earthquake Center.

Smith, B.R., and Sandwell, D.T., 2003, Coulomb stress accumulation along the San Andreas fault system: Journal of Geophysical Research, v. 108, no. B6, 2296, doi: 10.1029/2002JB002136.

Smith, B.R., and Sandwell, D.T., 2006, A model of the earthquake cycle along the San Andreas fault system for the last 1000 years: Journal of Geophysical Research, v. 111, B01405, doi: 10.1029/2005JB003703.

Spotila, J.A., and Sieh, K., 2000, Architecture of transpressional thrust faulting in the San Bernardino Mountains, southern California, from deformation of a deeply weathered surface: Tectonics, v. 19, p. 589–615, doi: 10.1029/1999TC001150.

Spotila, J.A., Farley, K.A., Yule, J.D., and Reiners, P.W., 2001, Near-field transpressive deformation along the San Andreas fault zone in southern California, based on exhumation constrained by (U-Th)/He dating: Journal of Geophysical Research, v. 106, no. B12, p. 30,909–30,922, doi: 10.1029/2001JB000348.

Spotila, J.A., Niemi, N., Brady, R., House, M., and Buscher, J., 2007, Long-term continental deformation associated with transpressive plate motion: The San Andreas fault: Geology, v. 35, p. 967–970, doi: 10.1130/G23816A.1.

Wald, D.J., and Heaton, T.H., 1994, Spatial and temporal distribution of slip for the Landers, California, earthquake: Seismological Society of America Bulletin, v. 84, p. 668–691.

Weldon, R.J., II, and Sieh, K., 1985, Holocene rate of slip and tentative recurrence interval for large earthquakes on the San Andreas fault, Cajon Pass, southern California: Geological Society of America Bulletin, v. 96, p. 793–812.

Weldon, R., Fumal, T., and Biasi, G., 2004, Wrightwood and the earthquake cycle: What a long recurrence record tells up about how faults work: GSA Today, v. 14, no. 9, doi: 10.1130/1052–5173(2004)014.

Weldon, R., Fumal, T., Biasi, G., and Sharer, K., 2005, Past and future earthquakes on the San Andreas fault: Science, v. 308, p. 966–967, doi: 10.1126/science.1111707.

Yule, D., and Sieh, K., 1997, Neotectonic and paleoseismic investigation of the San Andreas fault system, San Gorgonio pass: The 1996 Southern California Earthquake Center Annual Report: Progress Reports from SCEC scientists, v. 2, p. C.70–C.74.

Yule, D., and Sieh, K., 2003, Complexities of the San Andreas fault near San Gorgonio pass: Implications for large earthquakes: Journal of Geophysical Research, v. 109, no. B11, 2548, doi: 10.1029/2001JB000451.

Yule, J., Fumal, T., McGill, S., and Seitz, G., 2001, Active tectonics and paleoseismic record of the San Andreas fault, Wrightwood to Indio: Working toward a forecast of the next "Big Event", *in* Dunne, G., and Cooper, J., eds., Geologic excursions in the Californian deserts and adjacent Transverse Ranges: Los Angeles, California, Pacific Section, SEPM (Society for Sedimentary Geology), p. 91–126.

Manuscript received 27 April 2008
Revised manuscript received 29 September 2008
Manuscript accepted 9 October 2008

Printed in USA